

## **Analysis and comparison of different PV array configurations under partial shading conditions**

Dheeraj Soni (Department of Mechanical Engineering, SS College of Engineering, Udaipur, Raj, India)  
Piyush Sharma (Department of Electrical Engineering, SS College of Engineering, Udaipur, Raj, India)  
Nidhi Jain (Department of Basic Sc. & Humanities, SS College of Engineering, Udaipur, Raj, India)

### **ABSTRACT**

In the world, energy needs of people are met by fossil fuels. However, fossil fuels are getting depleted day by day and using of them causes negative effect on the environment. Moreover, energy demand of the world has increased in recent years. Hence, in order to meet the energy demand, especially solar or photovoltaic energy is widely used among the renewable energy sources. Photovoltaic cell directly convert solar energy into electricity. However, efficiency of photovoltaic cell is negatively affected by partial shading. Partial shading generally occurs on photovoltaic systems due to passing cloud, neighboring building, tree, etc. As a result of partial shading, produced power from photovoltaic system is less than the expected power value. One of the solutions of this problem is photovoltaic array configurations scheme. In this study, five different photovoltaic array configuration schemes: Series, Series-Parallel, Total-Cross-Tied, Bridged-Linked, and Honey-Comb, are carried out using 6×6 photovoltaic array under six different shading cases. Simulations of all shading cases are implemented using MATLAB/Simulink. In general, the obtained maximum power results under all partial shading cases show that Total-Cross-Tied configuration has the best performance according to other configurations. Furthermore, the obtained results have been compared in terms of shading loss, mismatch loss, and fill factor.

### **1. Introduction**

In the world, energy demand is increasing with the increase of human population. The majority of energy needs of human population are met by fossil fuels. However, fossil fuels are getting depleted and its damage to the environment is increasing day by day. Therefore, the use of renewable energy sources especially solar or photovoltaic (PV) energy is becoming widespread (Rao et al., 2014; Malathy and Ramaprabha, 2015; Pareek and Dahiya, 2016; Yadav et al., 2017; Bana and Saini, 2017). Solar energy is freely available, pollution-free, low maintenance cost, reliable, and infinite. However, it has some drawbacks such as the high installation cost and low energy conversion efficiency (Reisi et al., 2013; Subudhi and Pradhan, 2013; Bhatnagar and Nema, 2013; Pareek and Dahiya, 2016; Jazayeri et al., 2014). Electricity from solar energy is produced by PV cell. It has a nonlinear current–voltage (I–V) characteristic and there is a maximum power point (MPP) on its power–voltage (P–V) characteristic. The output power of PV module depends on solar irradiation and temperature. In order to improve the efficiency of PV module, it must be operated at the MPP (Reisi et al., 2013; Subudhi and Pradhan, 2013; Bhatnagar and Nema, 2013; Malathy and Ramaprabha, 2015). One of the major cause reducing the efficiency of PV module is partial shading (PS). Partial shading is caused by several factors such as cloud, building, tree, and snow (Wang and Hsu, 2010; Belhachat and Larbes, 2015; Bana and Saini, 2017). In partial shading conditions, PV modules of the array receive different solar irradiation values. Therefore, there are multiple peaks on the P-V and I-V characteristics of the PV array, so power losses occur in the

system. One of the solutions of reducing the power losses is PV array configurations schemes (Rao et al., 2014; Belhachat and Larbes, 2015; Yadav et al., 2017; Bana and Saini, 2017).

In the literature, different PV array configuration schemes are proposed such as Series (S), Parallel (P), Series-Parallel (SP), Total-Cross- Tied (TCT), Bridged-Linked (BL), and Honey-Comb (HC). El-Dein et al. (2013), proposed a novel mathematical formulation for finding the optimal reconfiguration of PV array as a mixed integer quadratic programming problem in order to reducing the partial shading losses. The PV array is constructed from the interconnection of PV modules in half reconfigurable PV array, full reconfigurable PV array, and TCT. The results of these configurations are compared and the authors found that the partial shading losses are reduced with the proposed reconfiguration. Rao et al. (2014) proposed a fixed interconnection scheme for PV arrays in order to improve the PV efficiency under partial shading conditions. This proposed scheme was implemented on  $3 \times 3$  PV array. The results of the proposed scheme were compared with the results of the SP, TCT, and BL configuration. Belhachat and Larbes (2015) analyzed the performance of S, P, SP, TCT, BL, and HC configurations under all possible scenarios of shading on  $6 \times 4$  PV array. The Bishop model of a photovoltaic module was used. The obtained results showed that TCT configuration provided the best performances under most cases of PSC. Malathy and Ramaprabha (2015) analyzed the performance of PV array configurations for different array sizes under different shading patterns. Moreover, they proposed new configuration as well as S, P, SP, TCT, HC, and BL. New configuration gave the better maximum power than TCT configurations. Pareek and Dahiya (2016), proposed a novel method to forecast the interconnection of modules in TCT configuration PV array. In novel method, the placement of shaded and non-shaded modules in array is done in such a way in order to distribute the shading effects evenly in each row. The study is realized under different shading scenarios. The results show that the method provides multiple solutions for reconfiguration of PV array in order to increase the efficiency of PV array. Bana and Saini (2017) proposed a novel PV array configuration under 14 shading scenarios. The output power of novel PV array configuration is compared with SP, TCT, BL, and HC configuration.

In this study, performance of S, SP, TCT, BL, and HC configurations was analyzed for different shading cases on  $6 \times 6$  PV array. Simulations of all PV array configurations under different shading cases were realized using MATLAB/Simulink. Performances of PV array configurations were compared in terms of maximum power value, shading loss, mismatch loss, and fill factor. The results show that TCT configuration gives better performance with highest maximum power, the lowest mismatch loss, and the highest fill factor than other PV array configurations.

This study is a review study for PV array configurations. In this study, all situations used in comparing the performances of the PV array configurations are explicitly given and explained for all PV array configurations contrary to other studies in the literature. The study has been carried out for S, SP, TCT, BL, and HC configurations given in the literature and a large size PV array was used instead of small size PV array. Under all possible partial shading conditions, the study was simulated and results were clearly given. The performance of all configurations was compared in terms of maximum power value, shading loss, mismatch loss, and fill factor.

This paper is organized as follows: Section 2 presents the mathematical model of PV cell and module and PV module characteristic under uniform and changing environmental conditions. In Section 3, PV array configurations are clearly explained. In Section 4, all the considered PV array configurations are analyzed

and compared in terms of maximum power value. In Section 5, performance of PV array configurations are compared with regard to shading loss, mismatch loss, and fill factor.

## 2. Mathematical model of PV

Various electrical equivalents of the PV cell are found in literature and the one diode model is the most widely used model among them. The equivalent circuit of one single diode model is shown in Fig. 1. The circuit consists of a photo current ( $I_{ph}$ ), a diode ( $D$ ), a parallel resistance ( $R_p$ ) representing the leakage

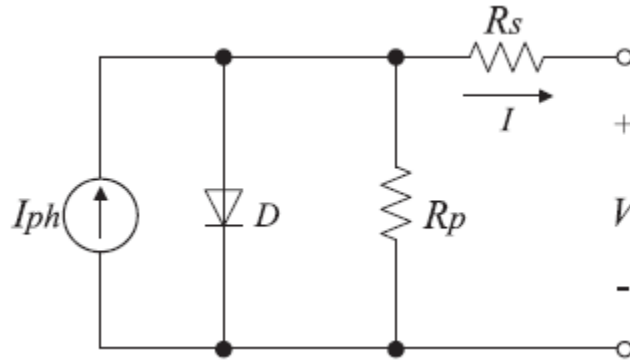


Fig. 1. The equivalent circuit of one diode model.

current and a series resistance ( $R_s$ ) representing an internal resistance of the PV cell (De Soto et al., 2006; Tsai et al., 2008; Villalva et al., 2009; Tsai, 2010). The voltage-current characteristic equation of a PV cell is given as follows

$$I = I_{ph} - I_0 \left[ \exp\left(\frac{q}{kTA}(V + IR_s)\right) - 1 \right] - \frac{V + IR_s}{R_p} \quad (1)$$

where  $I_{ph}$  is light generated current,  $I_0$  is the cell saturation of dark current,  $T$  is the cell's operating temperature in Kelvin (K),  $k$  is the Boltzmann constant ( $1.381 \times 10^{-23}$  J/K),  $q$  is the electron charge ( $1.602 \times 10^{-19}$  C),  $A$  is diode ideality constant (De Soto et al., 2006; Tsai et al., 2008; Villalva et al., 2009; Tsai, 2010). The photovoltaic current mainly depends on the solar irradiation and temperature given as

$$I_{ph} = [I_{sc} + K_I(T - T_{ref})]G/G_n \quad (2)$$

where  $I_{sc}$  is the short circuit current of the cell at 25 °C and 1000 W/m<sup>2</sup>,  $K_I$  is the short-circuit current temperature coefficient of the cell,  $T_{ref}$  is the reference temperature of the cell,  $G$  is the solar irradiation of the cell and  $G_n$  is the nominal solar irradiation in W/m<sup>2</sup> (De Soto et al., 2006; Tsai et al., 2008; Villalva et al., 2009; Tsai, 2010). The saturation current varies with the cell temperature and it can be expressed as

$$I_0 = I_{0,n} \left(\frac{T_{ref}}{T}\right)^3 \exp\left[\frac{qE_g}{Ak} \left(\frac{1}{T_{ref}} - \frac{1}{T}\right)\right] \quad (3)$$

where  $I_{0,n}$  is the nominal saturation current,  $E_g$  is the band gap energy of the semiconductor ( $E_g = 1.12$  eV for the polycrystalline Si at 25 °C).

The output power of a typical PV cell is less than 2 Watt (W) at 0.5 Volt (V). In order to produce desired output power, PV cells are connected in a module of series and parallel configuration (Tsai et al., 2008; Villalva et al., 2009; Tsai, 2010). The equivalent circuit of the PV module arranged in  $N_p$  parallel and  $N_s$  series is shown in Fig. 2. The voltage-current characteristic equation of a PV module is given in Eq. (4).

$$I = N_p I_{PH} - N_p I_0 \left[ \exp \left( \frac{q}{kTA} \left( \frac{V}{N_s} + \frac{IR_s}{N_p} \right) \right) - 1 \right] - \frac{\frac{N_p}{N_s} V + IR_s}{R_p} \quad (4)$$

Simulink model of PV module is given in Fig. 3. I-V and P-V characteristic of PV module used in the system are given in Fig. 4(a) and (b). PV module parameters used in the system is given in Table 1 (<https://www.solarelectricsupply.com/fileuploader/download/download/?d=0&file=custom%2Fupload%2FSES-450J-data-sheet.pdf>)

The output power of PV module mainly depends on solar irradiation and temperature. According to Eq. (2), the short circuit current of the PV module and solar irradiation are directly proportional to each other. Therefore, the power of the PV module is directly proportional to solar irradiation. When the solar irradiation level decreases, the power of the PV module decreases (Tsai et al., 2008; Villalva et al., 2009). I-V and P-V characteristic of PV module for different solar irradiation levels at constant temperature (25 °C) are shown in Fig. 5(a) and (b). According to Fig. 5(a), when the solar irradiation increases, the short circuit current of the PV module increases, so the power increases.

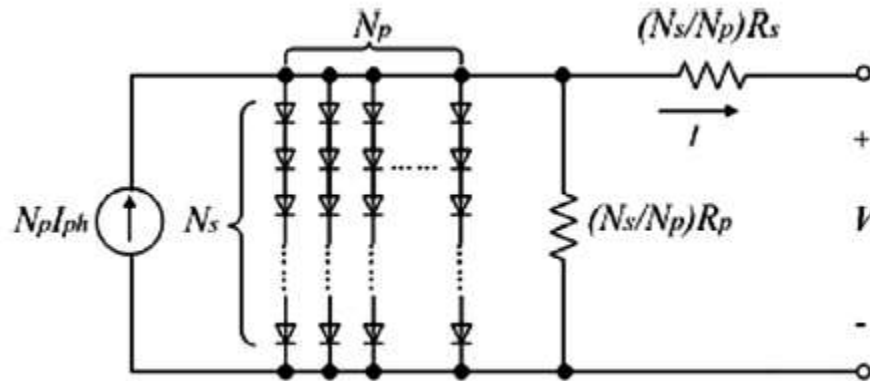


Fig. 2. The equivalent circuit of the PV module.

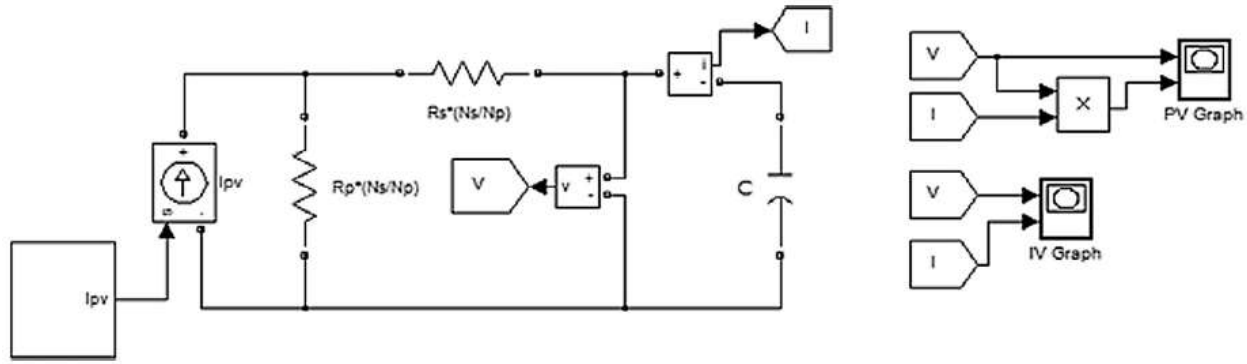


Fig. 3. Simulink model of PV module.

According to Eq. (3), the short-circuit current of the PV module and temperature are inversely proportional to each other. In other words, the power of the PV module is inversely proportional to solar irradiation. When the temperature increases, the power of the PV module decreases (Tsai et al., 2008; Villalva et al., 2009). I-V and P-V characteristic of PV module for different temperature at constant solar irradiation ( $1000 \text{ W/m}^2$ ) are shown in Fig. 6(a) and (b). According to Fig. 6(a), when the temperature decreases, the open circuit voltage of the PV module increases, so the power increases.

### 3. PV array configurations

Fig. 7 shows the schematic diagram of PV array configurations. Five different array configurations are reported in this paper. These are series (S), series-parallel (SP), total-cross-tied (TCT), bridged-link (BL), and honey-comb (HC).

S configuration is the simple and basic configuration and it is shown in Fig. 7(a). While output voltage of this configuration is high, but output current is low. Therefore, various configuration schemes are proposed so as to overcome this drawback (Malathy and Ramaprabha, 2015; Belhachat and Larbes, 2015; Amin et al., 2016; Bana and Saini, 2017).

SP configuration is shown in Fig. 7(b). In order to get desired output voltage, all modules are first connected in series form and then these series connection are connected in parallel (Malathy and Ramaprabha, 2015; Belhachat and Larbes, 2015; Bana and Saini, 2017; Pareek and Dahiya, 2016; Amin et al., 2016).

Table 1 PV module parameters used in the system.

Parameter	Variable	Value
Maximum power	$P_{max}$	50 W
Maximum power point voltage	$V_{mpp}$	17.5 V
Maximum power point current	$I_{mpp}$	2.9 A
Open circuit voltage	$V_{oc}$	21.8 V
Short circuit current	$I_{sc}$	3.2 A
Number of series cell	$N_s$	72
Temperature coefficient of $I_{sc}$	$K_1$	0.105%/°C

TCT configuration is shown in Fig. 7(c). It is derived from SP configuration by connected cross ties across each row of the modules. In this configuration, the voltage across the each row is equal and the sum of current across the each column is equal (Malathy and Ramaprabha, 2015; Belhachat and Larbes, 2015; Pareek and Dahiya, 2016; Amin et al., 2016; Bana and Saini, 2017).

BL configuration is shown in Fig. 7(d). There is a bridged unit with four modules. Two modules in a bridge are connected in series and then they are connected in parallel. Bridges are linked via cross ties (Malathy and Ramaprabha, 2015; Belhachat and Larbes, 2015; Pareek and Dahiya, 2016; Bana and Saini, 2017).

HC configuration is shown in Fig. 7 (e). HC is a modified version of BL configuration and its bridge size is variable (Malathy and Ramaprabha, 2015; Belhachat and Larbes, 2015; Bana and Saini, 2017).

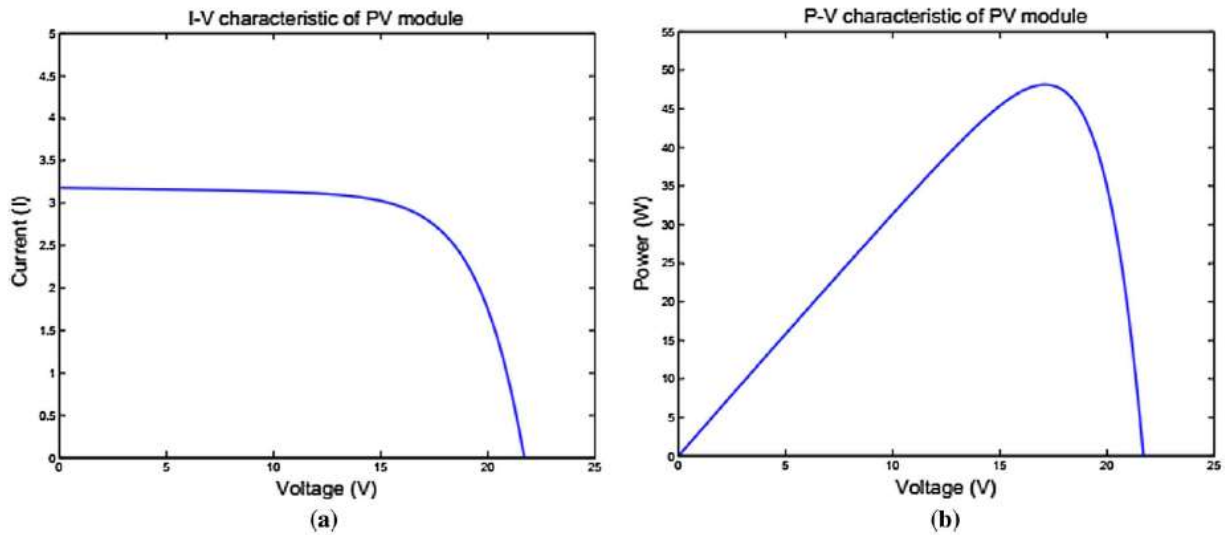


Fig. 4. (a) I-V, (b) P-V characteristic of PV module.

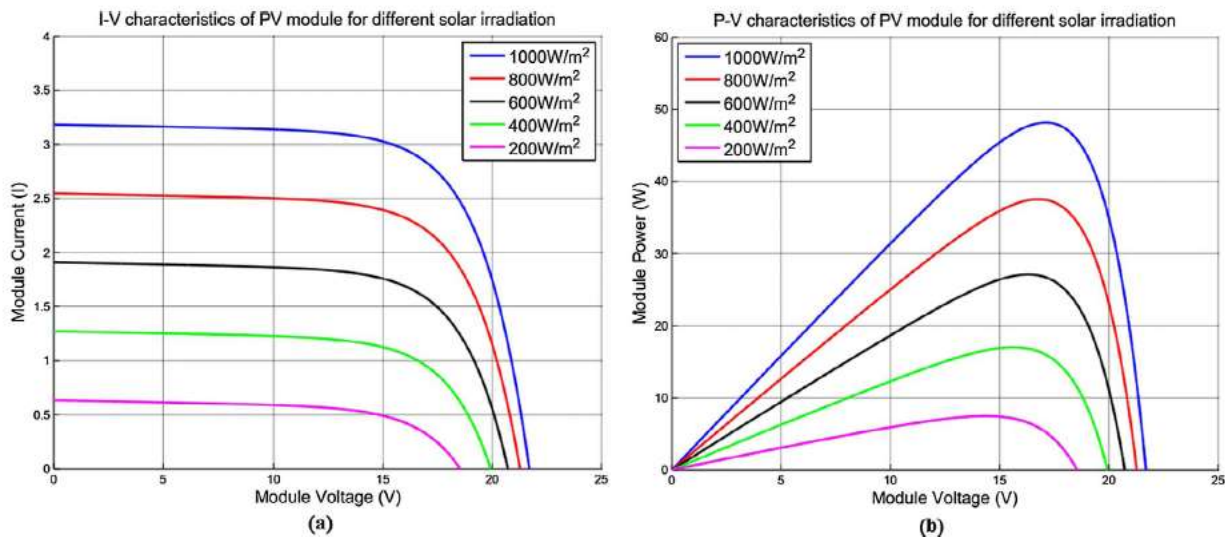


Fig. 5. (a) I-V and (b) P-V characteristic of PV module for different solar irradiation.

#### 4. Analysis of partial shading conditions

I-V and P-V characteristic of all PV array configurations at uniform condition ( $1000 \text{ W/m}^2$  at  $25^\circ\text{C}$ ) are given in Fig. 8(a) and (b), respectively. In Table 2, maximum power for all PV array configurations for a  $6 \times 6$  array is given. According to Table 2, S, SP, TCT, BL, and HC configurations gives the same maximum power at uniform condition.

In order to investigate the efficiency of PV array configurations, we have conducted our tests on  $6 \times 6$  PV array under partial shading conditions. Moreover, all shading cases are carried out  $25^\circ\text{C}$ . Shading values of cases are three different solar irradiation values:  $300 \text{ W/m}^2$ ,  $600 \text{ W/m}^2$ , and  $1000 \text{ W/m}^2$ . The partial shading cases used in this study are given in Fig. 9.

Case 1. The solar irradiance value of the first column is  $300 \text{ W/m}^2$ , the second and the third column is  $600 \text{ W/m}^2$ , and other columns are  $1000 \text{ W/m}^2$ . Case 1 is shown in Fig. 9(a).

Case 2. The solar irradiance values of the half of first and second column from top are  $300 \text{ W/m}^2$ , the half of fifth and sixth column from bottom is  $600 \text{ W/m}^2$ , and other modules are  $1000 \text{ W/m}^2$ . Case 2 is shown in Fig. 9(b).

Case 3. The solar irradiance values of the diagonal of the array are  $300 \text{ W/m}^2$ , modules in the neighborhood of the diagonal of the array are  $600 \text{ W/m}^2$ , and other modules are  $1000 \text{ W/m}^2$ . Case 3 is shown in Fig. 9(c).

Case 4. The solar irradiance values of the four modules at the middle of the array are  $300 \text{ W/m}^2$ , modules in the neighborhood of the diagonal of the four modules are  $600 \text{ W/m}^2$ , and other modules are  $1000 \text{ W/m}^2$ . Case 4 is shown in Fig. 9(d).

Case 5. The solar irradiance values of the corner of the PV array are  $300 \text{ W/m}^2$ , modules in the neighborhood of the corner are  $600 \text{ W/m}^2$ , and other modules are  $1000 \text{ W/m}^2$ . Case 5 is shown in Fig. 9(e).

Case 6. The solar irradiance values PV array is randomly distributed. Case 6 is shown in Fig. 9(f).

Simulation results of shading cases are given in Table 3.

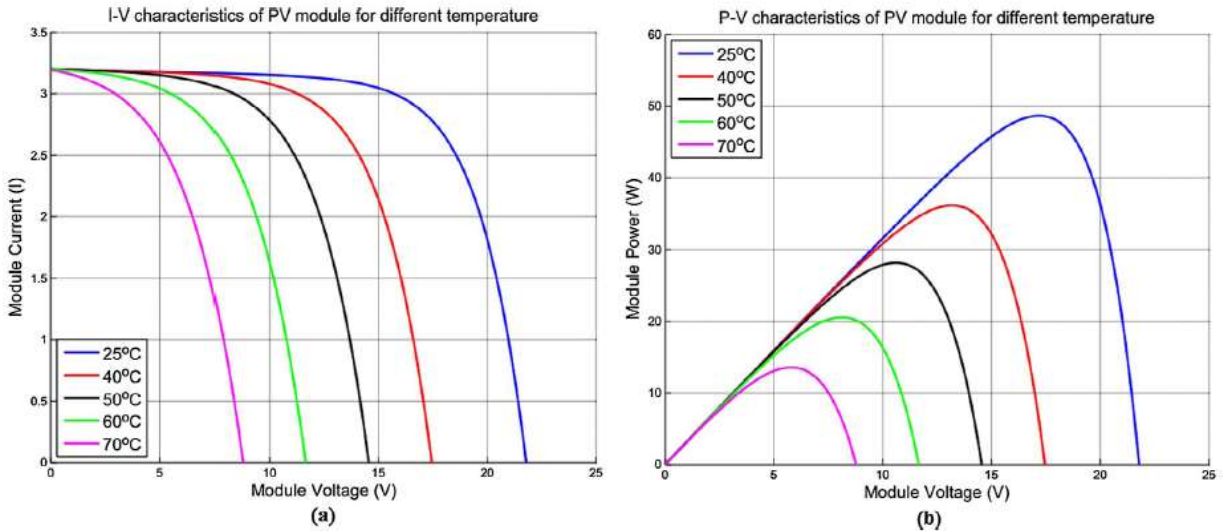


Fig. 6. (a) I-V and (b) P-V characteristic of PV module for different temperature.

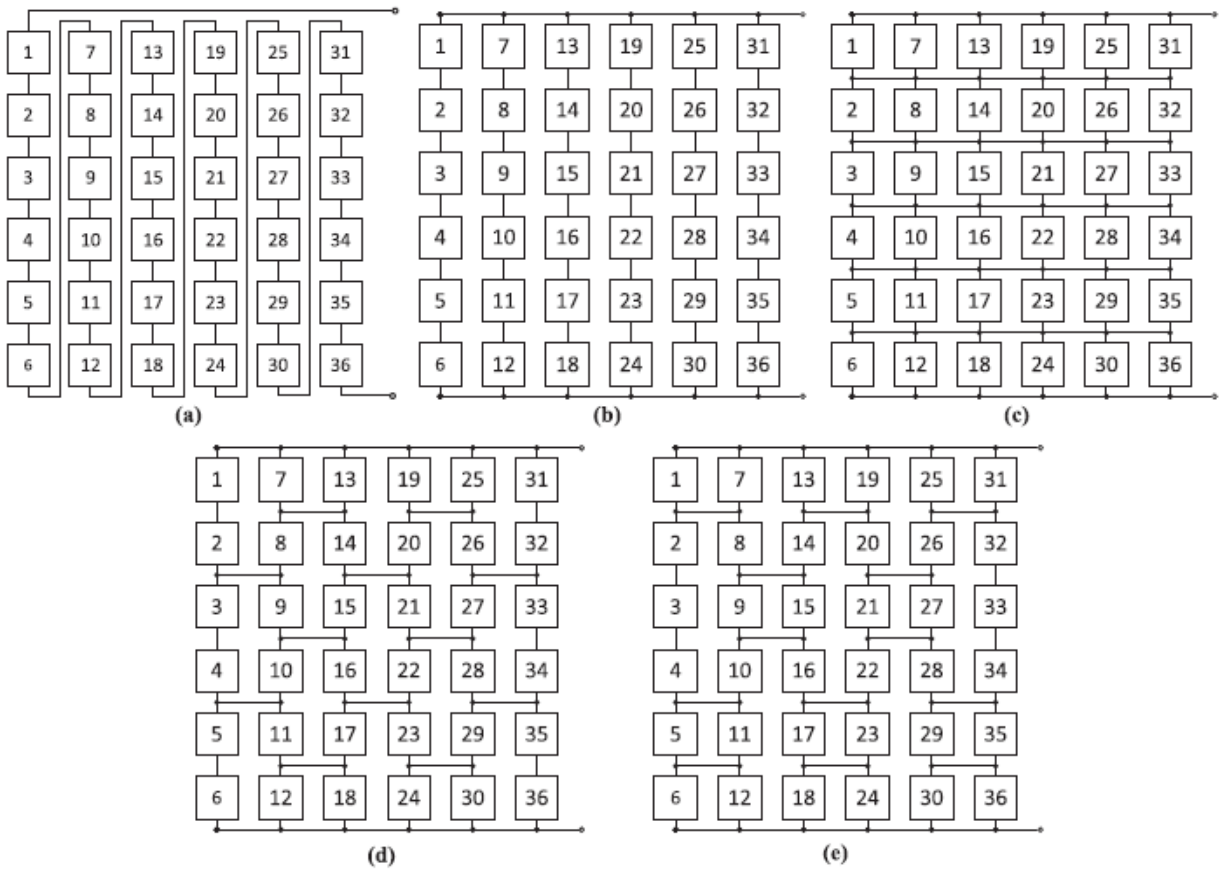


Fig. 7. The schematic diagram of PV array configurations (a) S, (b) SP, (c) TCT, (d) BL, (e) HC.

According to Table 3, the following results were obtained.

For Case 1, the configurations S, SP, TCT, BL and HC provide the same maximum power. They show the highest maximum power (1242 W) with respect to maximum power of S (941.3655 W) configuration.

For Case 2, TCT configuration gives the highest maximum power (1340.4 W). The BL configuration has second best maximum power (1176.8 W) but SP configuration has the lowest maximum power (1112.2 W).

Table 2 Maximum power for all pv array configurations for a 6×6 array.

Configuration	$P_{max}$ (W)	$V_{max}$ (V)	$I_{max}$ (A)
S	1733	612.6	2.829
SP	1733	102.1	16.98
TCT	1733	102.1	16.98
BL	1733	102.1	16.98
HC	1733	102.1	16.98

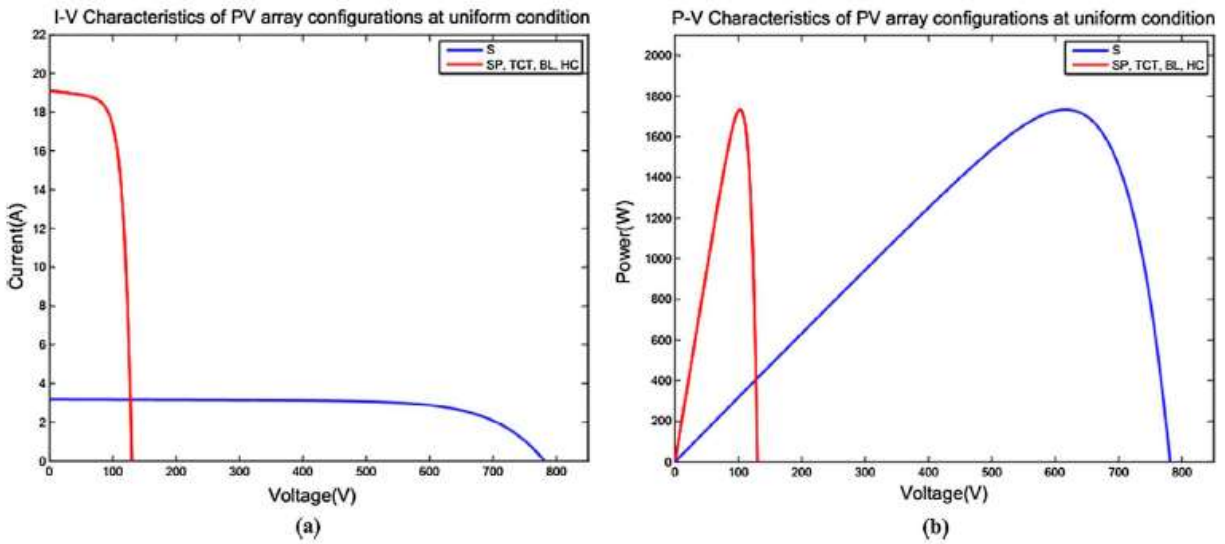


Fig. 8. (a) I-V and (b) P-V characteristic of PV array configurations at uniform condition.

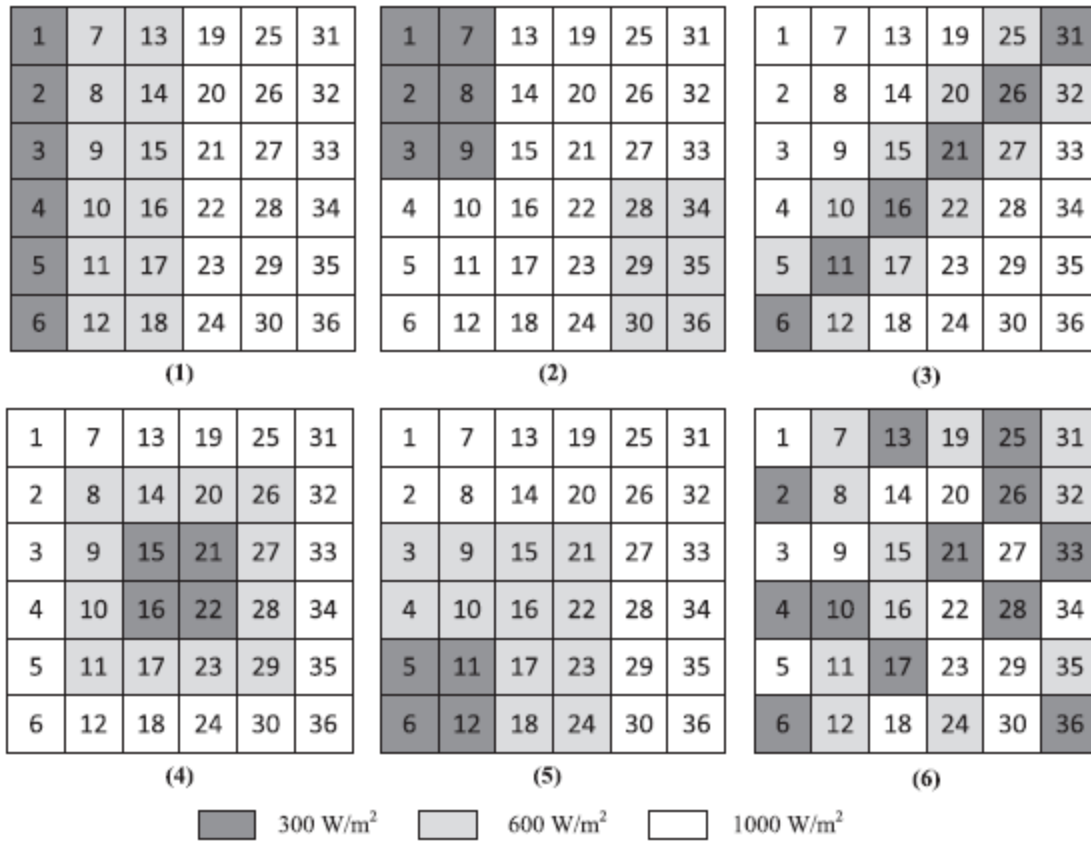


Fig. 9. Partial shading (a) Case 1, (b) Case 2, (c) Case 3, (d) Case 4, (e) Case 5, (f) Case 6.

Table 3 Simulation results of shading cases. The bold values show the maximum values.

	Configuration	$P_{max}$ (W)	$V_{max}$ (V)	$I_{max}$ (A)
Case 1	S	941.3655	530.1	1.776
	SP	<b>1242</b>	<b>97.5</b>	<b>12.74</b>
	TCT	<b>1242</b>	<b>97.5</b>	<b>12.74</b>
	BL	<b>1242</b>	<b>97.5</b>	<b>12.74</b>
	HC	<b>1242</b>	<b>97.5</b>	<b>12.74</b>
Case 2	S	1128	401.3	2.811
	SP	1112.2	102.3	10.87
	TCT	<b>1340.4</b>	<b>99.61</b>	<b>13.46</b>
	BL	1176.8	106	11.09
	HC	1164.1	105.01	11.07
Case 3	S	555.1542	633.2	0.877
	SP	725.748	87.75	8.271
	TCT	<b>898.2565</b>	<b>100.3</b>	<b>8.954</b>
	BL	734.5931	85.3	8.612
	HC	774.7161	101.3	7.645
Case 4	S	1015.2	573.9	1.765
	SP	1103.4	104.6	10.55
	TCT	<b>1163.2</b>	<b>104.3</b>	<b>11.15</b>
	BL	1106.8	103.9	10.65
	HC	1134	103.7	10.93
Case 5	S	1005.8	566.8	1.774
	SP	1096.2	103.7	10.57
	TCT	<b>1159.3</b>	<b>104.3</b>	<b>11.12</b>
	BL	1116.1	104.5	10.68
	HC	1102.3	103.6	10.64
Case 6	S	729.9984	415.5	1.759
	SP	682.9867	48.96	13.95
	TCT	<b>1002.2</b>	<b>101.3</b>	<b>9.885</b>
	BL	732.2328	103.9	7.045
	HC	742.4291	104.5	7.105

The bold values show the maximum values.

For Case 3, TCT configuration presents the best performance with the highest maximum power (898.2565 W). It is followed by the HC configuration (774.7161 W). The S configuration presents the lowest performance (555.1542 W).

For Case 4, TCT configuration provides the highest maximum power (1163.2 W). It is followed by the HC configuration (1134 W). The S configuration presents the lowest performance (1015.2 W). For Case 5, TCT configuration gives the highest maximum power (1159.3 W). The BL configuration comes second best (1116.1 W), but S configuration has the lowest maximum power (1005.8 W). For Case 6, TCT configuration presents the best performance with the highest maximum power (1002.2 W). It is followed by the HC configuration (742.4291 W). The SP configuration presents the lowest performance (682.9867 W).

## 5. Results and discussion

Maximum powers of each case for PV array configurations are compared. As a result, SP, TCT, BL, and HC configurations have the same maximum power for the Case 1. For other shading cases, the highest power is obtained from TCT configurations. Moreover, the results of shading cases are compared in terms

of mismatch loss, shading loss, and fill factor. In Fig. 10, Shading and mismatch losses for a PV array are shown.

### 5.1. Shading loss

Shading loss is the difference between the array maximum power without partial shading and the sum of individual maximum power of the modules under partial shading condition (El-Dein et al., 2013; Vijayalekshmy et al., 2014, 2016). Shading loss is computed by Eq. (5).

$$P_{\text{shadingloss}} = P_{\text{max}_u} - P_{\text{max}_i} \quad (5)$$

In Eq. (5),  $P_{\text{shadingloss}}$ ,  $P_{\text{max}_u}$ , and  $P_{\text{max}_i}$  are represents the shading loss, maximum power under uniform condition, and sum of individual maximum power of the modules, respectively. The array maximum power under uniform condition is 1733W for all configurations. Moreover, the sum of individual maximum powers of the modules is given in Table 4. For each case,  $P_{\text{max}_i}$  is same for PV array configurations. In Table 5, shading loss values of all configurations are given. According to Table 5, for each shading cases, all configurations give the same shading loss. Shading loss for five different configurations is shown in Fig. 11.

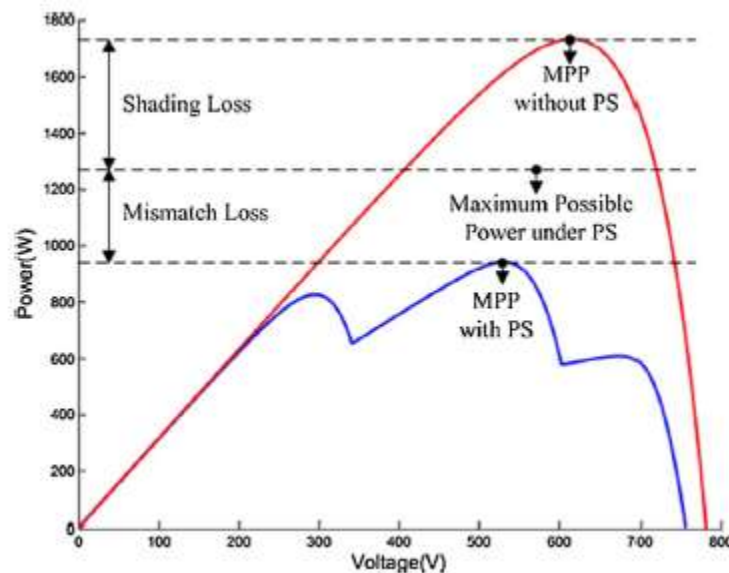


Fig. 10. Shading and mismatch losses for a PV array.

Table 4 The sum of individual maximum powers of the modules

Cases	$P_{\text{max}_i}$
Case 1	1264.7718 W
Case 2	1391.0394 W
Case 3	1306.8610 W
Case 4	1336.7776 W
Case 5	1336.7776 W
Case 6	1069.799 W

Table 5 Shading loss (W) values of all configurations.

	Case 1	Case 2	Case 3	Case 4	Case 5	Case 6
S	468.2282	341.961	426.139	366.2224	366.2224	663.2010
SP	468.2282	341.961	426.139	366.2224	366.2224	663.2010
TCT	468.2282	341.961	426.139	366.2224	366.2224	663.2010
BL	468.2282	341.961	426.139	366.2224	366.2224	663.2010
HC	468.2282	341.961	426.139	366.2224	366.2224	663.2010

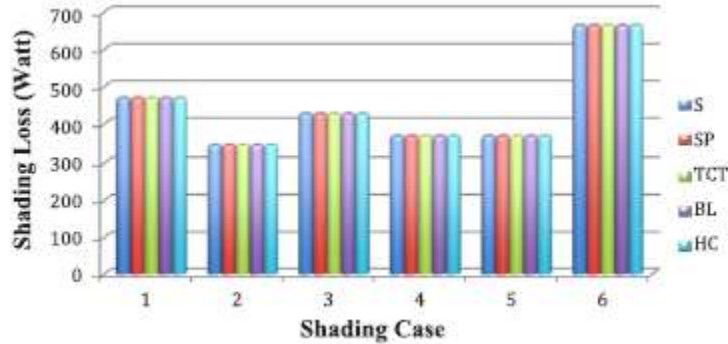


Fig. 11. Shading loss for five different configurations.

Table 7 Mismatch loss (%) values of all configurations.

	Case 1	Case 2	Case 3	Case 4	Case 5	Case 6
S	25.57	18.91	57.52	25.72	26.41	31.76
SP	<b>1.80</b>	19.96	44.47	19.27	19.80	35.50
TCT	<b>1.80</b>	<b>3.38</b>	<b>31.27</b>	<b>14.89</b>	<b>15.18</b>	<b>6.32</b>
BL	<b>1.80</b>	15.40	43.79	19.02	18.34	31.55
HC	<b>1.80</b>	16.31	40.72	17.03	19.35	30.60

The bold values show the maximum values.

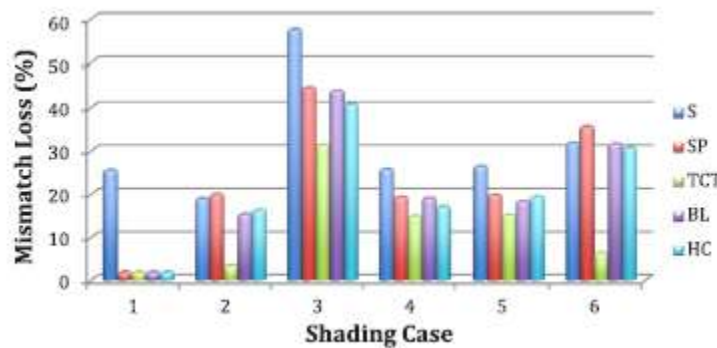


Fig. 12. Mismatch loss (%) for five different configurations.

Table 8 The open circuit voltage and short circuit current of configurations.

Cases		S	SP	TCT	BL	HC
Case 1	V <sub>OC</sub> (V)	755.3385	126.9222	126.9222	126.9222	126.9222
	I <sub>SC</sub> (A)	3.1776	14.3045	14.3045	14.3045	14.3045
Case 2	V <sub>OC</sub> (V)	761.3249	127.3539	127.8442	127.5659	127.6148
	I <sub>SC</sub> (A)	3.18	10.72	13.1	11.14	11.07
Case 3	V <sub>OC</sub> (V)	737.2133	123.1807	124.0789	123.4	123.68
	I <sub>SC</sub> (A)	1.8807	16.4147	12.8124	15.09	16.2858
Case 4	V <sub>OC</sub> (V)	760.272	127.1317	127.2871	127.1352	127.1983
	I <sub>SC</sub> (A)	3.1787	19.005	19.0312	19.0104	19.0312
Case 5	V <sub>OC</sub> (V)	758.7139	126.9824	127.0812	127.0716	127.0117
	I <sub>SC</sub> (A)	2.9875	18.9782	18.9378	19	18.9278
Case 6	V <sub>OC</sub> (V)	742.134	123.7934	125.062	124.165	124.5377
	I <sub>SC</sub> (A)	3.1739	18.9636	14.1677	18.9377	16.3646

Table 9 Fill factor values of all configurations.

	Case 1	Case 2	Case 3	Case 4	Case 5	Case 6
S	0.39	0.47	0.40	0.42	0.44	0.31
SP	<b>0.68</b>	0.46	0.36	0.46	0.45	0.29
TCT	<b>0.68</b>	<b>0.64</b>	<b>0.57</b>	<b>0.48</b>	<b>0.48</b>	<b>0.57</b>
BL	<b>0.68</b>	0.49	0.39	0.46	0.46	0.31
HC	<b>0.68</b>	0.48	0.38	0.47	0.46	0.36

The bold values show the maximum values.

Table 6 The global maximum power point of all configurations.

	Case 1	Case 2	Case 3	Case 4	Case 5	Case 6
S	941.3655 W	1128 W	555.2242 W	1015.2 W	1005.8 W	729.9938 W
SP	1242 W	1113.3 W	725.748 W	1103.4 W	1096.2 W	690.0727 W
TCT	1242 W	1344 W	898.2565 W	1163.2 W	1159.3 W	1002.2 W
BL	1242 W	1176.8 W	734.5931 W	1106.8 W	1116.1 W	732.2328 W
HC	1242 W	1164.1 W	774.7161 W	1134 W	1102.3 W	742.4291 W

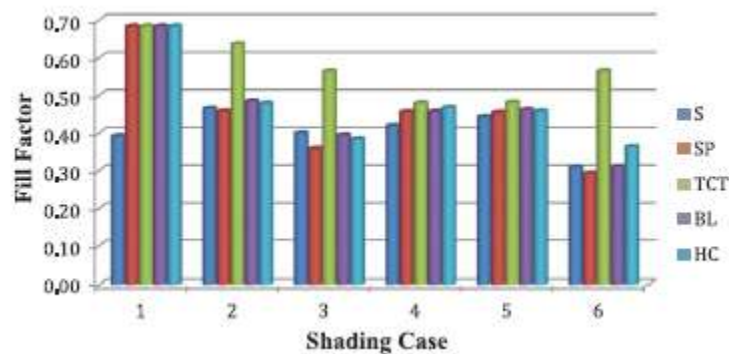


Fig. 13. Fill factor for five different configurations.

## 5.2. Mismatch loss

Mismatch loss is the difference between the sum of individual maximum power of the modules and the global maximum power point under partial shading conditions (Vijayalekshmy et al., 2014, 2016). Mismatch loss is computed by Eq. (6).

$$P_{\text{mismatchloss}} = P_{\text{max}_i} - P_{\text{GMPP}} \quad (6)$$

In Eq. (6),  $P_{\text{mismatchloss}}$ ,  $P_{\text{max}_i}$ , and  $P_{\text{GMPP}}$  are represents the mismatch loss, the sum of individual maximum power of the modules, and global maximum power point under partial shading conditions, respectively. For all shading cases, the global maximum power point of configurations are given in Table 6. Mismatch loss (%) values for all configurations is given in Table 7. According to Table 7, for Case 1, SP, TCT, BL, and HC give the same mismatch loss. For other shading cases, the mismatch loss is found to be lower in TCT configuration. In Fig. 12, mismatch loss (%) for five different configurations is given.

### 5.3. Fill factor

Fill factor (FF) is ratio of global maximum power to product of the open circuit voltage and short circuit current of the array configuration under the partial shading conditions (Vijayalekshmy et al., 2014, 2016). The fill factor is given in Eq. (7).

$$FF = \frac{P_{\text{GMPP}}}{V_{\text{oc}} \times I_{\text{sc}}} \quad (7)$$

In Eq. (7),  $P_{\text{GMPP}}$ ,  $V_{\text{OC}}$ , and  $I_{\text{SC}}$  represent the global maximum power point under partial shading conditions, open circuit voltage of array, and short circuit current of array, respectively. All shading cases, the open circuit voltage and short circuit current of configurations are given in Table 8. Fill factor values of all configurations is given in Table 9. For Case 1, SP, TCT, BL, and HC has the same fill factor value. The other shading cases, TCT has more fill factor values than other configurations. Fill factor for five different configurations is given in Fig. 13.

### 6. Conclusion

In this study, a comprehensive study which considers S, SP, TCT, BL, and HC PV array configurations has been carried out under six partial shading cases. For this purpose, simulations of all configurations for different shading cases has been implemented on 6×6 PV array using MATLAB/Simulink. Under uniform condition, all PV array configurations give the same maximum power. However, under partial shading conditions, performances of PV array configurations are different and depend on the shading case. For Case 1, TCT, SP, TCT, BL, and HC gives the highest maximum power (1242 W) and S gives the lowest maximum power (941.3655 W). When compared the S configuration, maximum power increase of the TCT, SP,TCT, BL, and HC configuration is 31.93%. For Case 2, TCT provides the highest maximum power (1340.4 W) and SP gives the lowest maximum power (1112.2 W). When compared the SP configuration, increase of maximum power value of the TCT configuration is 20.51%. For Case 3, TCT provides the highest maximum power (898.2565 W) and S gives the lowest maximum power (555.1542 W). When compared the S configuration increase of maximum power value of the TCT configuration is 61.8%. For Case 4, TCT provides the highest maximum power (1163.2 W) and S gives the lowest maximum power (1015.2 W). When compared the S configuration, increase of maximum power value of the TCT configuration is 14.57%. For Case 5, TCT presents the highest maximum power

(1159.3 W) and S gives the lowest maximum power (1005.8 W). When compared the S configuration, increase of maximum power value of the TCT configuration is 15.26%. For Case 6, TCT gives the highest maximum power (1002.2 W) SP gives the lowest maximum power (682.9867 W). When compared the SP configuration, increase of maximum power value of the TCT configuration is 46.74%.

According to these results, TCT provides the best performance for all shading conditions and it increases the maximum power compared to other configurations. Moreover, shading loss, mismatch loss, and fill factor has been compared for all PV array configurations. According to results, shading loss is the same for all configurations for each shading cases. TCT has the lowest mismatch loss and fill factor. As a result, efficiency of PV array strongly depends on the PV array configuration. Furthermore, shading cases, solar irradiation level, and type of shading case affect the efficiency of PV array.

#### References

- Amin, M., Bailey, J., Tapia, C., Thodimeladine, V., 2016. Comparison of PV array configuration efficiency under partial shading condition. In: IEEE 43rd Photovoltaic Specialists Conference (PVSC), 2016, pp. 3704–3707.
- Bana, S., Saini, R.P., 2017. Experimental investigation on power output of different photovoltaic array configurations under uniform and partial shading scenarios. *Energy* 127, 438–453.
- Belhachat, F., Larbes, C., 2015. Modeling, analysis and comparison of solar photovoltaic array configurations under partial shading conditions. *Sol. Energy* 120, 399–418.
- Bhatnagar, P., Nema, R.K., 2013. Maximum power point tracking control techniques: state-of-the-art in photovoltaic applications. *Renew. Sustain. Energy Rev.* 23, 224–241.
- De Soto, W., Klein, S.A., Beckman, W.A., 2006. Improvement and validation of a model for photovoltaic array performance. *Sol. Energy* 80 (1), 78–88.
- El-Dein, M.S., Kazerani, M., Salama, M.M.A., 2013. Optimal photovoltaic array reconfiguration to reduce partial shading losses. *IEEE Trans. Sustain. Energy* 4 (1), 145–153.
- Jazayeri, M., Uysal, S., Jazayeri, K., 2014. A comparative study on different photovoltaic array topologies under partial shading conditions. In: T&D Conference and Exposition, 2014 IEEE PES, pp. 1–5.
- Malathy, S., Ramaprabha, R., 2015. Comprehensive analysis on the role of array size and configuration on energy yield of photovoltaic systems under shaded conditions. *Renew. Sustain. Energy Rev.* 49, 672–679.
- Pareek, S., Dahiya, R., 2016. Enhanced power generation of partial shaded photovoltaic fields by forecasting the interconnection of modules. *Energy* 95, 561–572.
- Rao, P.S., Ilango, G.S., Nagamani, C., 2014. Maximum power from PV arrays using a fixed configuration under different shading conditions. *IEEE J. Photovoltaics* 4 (2), 679–686.
- Reisi, A.R., Moradi, M.H., Jamasb, S., 2013. Classification and comparison of maximum power point tracking techniques for photovoltaic system: a review. *Renew. Sustain. Energy Rev.* 19, 433–443.

- Subudhi, B., Pradhan, R., 2013. A comparative study on maximum power point tracking techniques for photovoltaic power systems. *IEEE Trans. Sustain. Energy* 4 (1), 89–98.
- Tsai, H.L., 2010. Insolation-oriented model of photovoltaic module using Matlab/Simulink. *Sol. Energy* 84 (7), 1318–1326.
- Tsai, H.L., Tu, C.S., Su, Y.J., 2008. Development of generalized photovoltaic model using MATLAB/SIMULINK. In: *Proceedings of the World Congress on Engineering and Computer Science*, pp. 1–6.
- Vijayalekshmy, S., Bindu, G.R., Iyer, S.R., 2016. A novel Zig-Zag scheme for power enhancement of partially shaded solar arrays. *Sol. Energy* 135, 92–102.
- Vijayalekshmy, S., Bindu, G.R., Iyer, S.R., 2014. Estimation of power losses in photovoltaic array configurations under moving cloud conditions. In: *Fourth International Conference on Advances in Computing and Communications (ICACC)*, 2014. IEEE, pp. 366–369.
- Villalva, M.G., Gazoli, J.R., Ruppert Filho, E., 2009. Comprehensive approach to modeling and simulation of photovoltaic arrays. *IEEE Trans. Power Electron.* 24 (5), 1198–1208.
- Yadav, A.S., Pachauri, R.K., Chauhan, Y.K., Choudhury, S., Singh, R., 2017. Performance enhancement of partially shaded PV array using novel shade dispersion effect on magic square puzzle configuration. *Sol. Energy* 144, 780–797.
- Wang, Y.J., Hsu, P.C., 2010. Analytical modelling of partial shading and different orientation of photovoltaic modules. *IET Renew. Power Gener.* 4 (3), 272–282.